



AIAS 2017 International Conference on Stress Analysis, AIAS 2017, 6–9 September 2017, Pisa, Italy

Experimental study of hydrogen embrittlement in Maraging steels

M. Barsanti^{a,b}, M. Beghini^a, F. Frascioni^b, R. Ishak^a, B. D. Monelli^a, R. Valentini^{a,b,*}

^aUniversità di Pisa, Dipartimento di Ingegneria Civile e Industriale, 56122 Pisa, Italy

^bINFN Sezione di Pisa, Largo Pontecorvo 2, 56125 Pisa, Italy

Abstract

This research activity aims at investigating the hydrogen embrittlement of Maraging steels in connection to real sudden failures of some of the suspension blades of the Virgo Project experimental apparatus. Some of them failed after 15 years of service in working conditions. Typically, in the Virgo detector, blades are loaded up to 50-60% of the material yield strength. For a deeper understanding of the failure, the relationship between hydrogen concentration and mechanical properties of the material, have been investigated with specimens prepared in order to simulate blade working conditions. A mechanical characterization of the material has been carried out by standard tensile testing in order to establish the effect of hydrogen content on the material strength. Further experimental activity was executed in order to characterize the fracture surface and to measure the hydrogen content. Finally, some of the failed blades have been analyzed in DICI-UNIPI laboratory. The experimental results show that the blades failure can be related with the hydrogen embrittlement phenomenon.

Copyright © 2018 The Authors. Published by Elsevier B.V.

Peer-review under responsibility of the Scientific Committee of AIAS 2017 International Conference on Stress Analysis

Keywords: Hydrogen embrittlement; Maraging; fracture analysis.

1. Introduction

Purpose of this work is the study of Hydrogen embrittlement of Maraging steel. Maraging is a class of Ultra High Strength Steels (UHSS) with a yield strength that can reach 2400 MPa, hardened by precipitation of intermetallic compounds during an aging process [Sha and Guo (2009)]. These steels are highly susceptible to hydrogen damage, as is common for high-strength alloys.

Maraging steel is the material used for the construction of some crucial components of the Virgo experiment [Beccaria et al. (1998)], like the blades of the suspension system of the interferometer mirrors (super-attenuators) shown in Fig. 1. The loads acting on the blades are very strong, because each filter must carry the weight of the underlying ones. Therefore these high loads can cause microcreep [Gurewitz et al. (1977)], that is present also in the

* R. Valentini Tel.: +39-50-221-7859 ; fax: +39-50-221-8065.

E-mail address: renzo.valentini@unipi.it

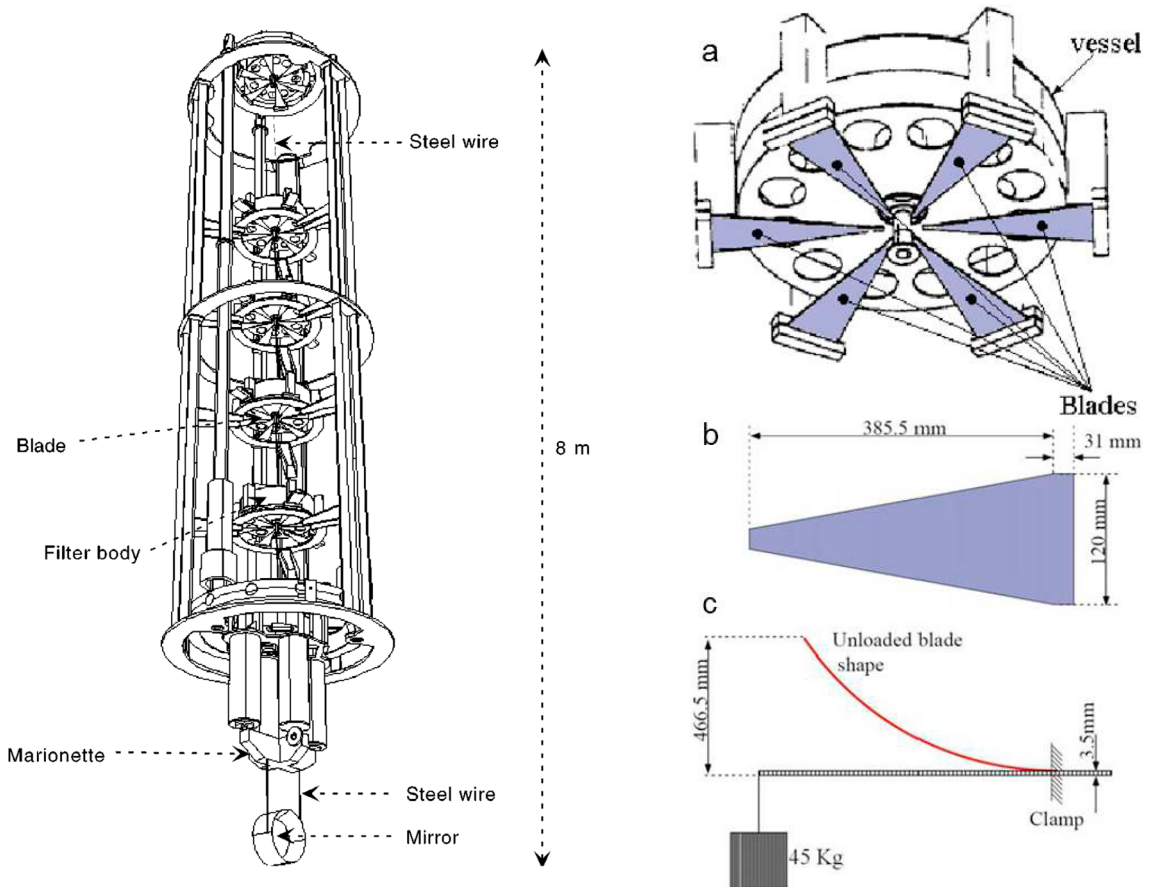


Fig. 1. The seismic super attenuator chain of Virgo (from Braccini et al. (2000)). The blades (b, c on the right) are clamped on the outer circumference of the filter bottom part (a on the right).

elastic regime. As the creep permanently modifies the position of the mirror and influences the measurement, a very high yielding strength was imposed.

Since nickel plating by surface deposition can produce hydrogen absorption, the possibility that this phenomenon could affect the mechanical properties of the Maraging steel used in the Virgo project has been investigated.

2. Material and methods

2.1. Material

This study examined a commercially available Maraging steel (Marval 18 produced by Aubert & Duvall) whose chemical composition is reported in table 1. The material was supplied as plates 3.4 mm thick. To improve its mechanical properties, the material has undergone an aging treatment (100 hours @435 °C). The values of the most important mechanical properties are shown in table 2.

Four groups of samples were prepared and studied as follows:

1. Failed blades: hydrogen content was measured.
2. Specimens with nickel electroless plating to simulate the plating procedure adopted for blade surface finishing, without de-hydrogenation treatment. Hydrogen content and mechanical properties were measured. This group helps to check the effect of missed steps in the adopted plating procedure for the blades.

Table 1. Chemical composition of the Maraging steel Marval 18.

Elements % in the alloy											
C	Ni	Co	Mo	Ti	Al	Si	Mn	P	Zr	B	S
<0,010	18,43	8,21	4,71	0,46	0,10	0,04	0,02	<0,005	0,004	0,0025	<0,002

Table 2. Mechanical properties of the Maraging steel Marval 18.

Mechanical properties	As received	Aged (100 h, 435 °C)
$R_{p0,2}$ [MPa]	870	1950
UTS [MPa]	1070	2030
Elongation [%]	14	7

3. Samples charged in NaOH 0.1 N de-aerated solution at cathodic current density in the range 0.1–1 mA/cm² for 160 hours. This group mimics low hydrogen content in the specimens. Both Hydrogen content and mechanical properties were measured for these specimens.
4. Samples charged in 3% NaCl + 0.3% NH₄SCN at cathodic current density of 0.2 mA/cm² for 160 hours to mimic high values of hydrogen content. Both hydrogen content and mechanical properties were measured for these specimens.

Before charging, each of the samples was treated in order to remove the oxide layer from the surfaces, so as to obtain a uniform surface. For this operation a series of abrasive papers have been used, starting from the coarsest granulometry and passing on to the finest granulometry. This phase is crucial as the Hydrogen charging procedure is strongly influenced by the superficial state of the sample.

The electrolytic cell consists of a closed beaker containing the solution, the metallic sample constituting the cathode, and a counterelectrode; both electrodes are connected to the potentiostat working in galvanostatic conditions. This scheme was used for all charging conditions. Having to charge more specimens in the same electrolytic cell, it was necessary to verify that each electrode was under the same conditions. Therefore, the charging procedure was conducted as follows:

1. Mounting the cell with a counter-electrode and a single Maraging sample, setting the current corresponding to the desired value for that sample, with potentiostat in galvanostatic mode;
2. Measuring of the potential between the test and reference electrode;
3. Setting the working conditions to potentiostatic mode, and the potential to the value measured in step 2;
4. inserting the other metal samples, connected in parallel with each other. The potentiostat increases proportionally the current when the number of sample is increased;
5. Verification of the effective current density by means of an amperometer.

2.2. Hydrogen concentration measurements

Hydrogen content of the received blades and charged samples was determined using LECO DH603 hydrogen determinator instrument. The charging conditions of the samples are described in the subsection 2.1. At the end of each charging procedure, a portion of the sample (approximately 50×10×3.5 mm) was cut, cleaned with ethanol, dried with cold air and weighed. The tests were performed at 1000°C for 15 min.

2.3. Mechanical testing

The tensile test allows to quantify the mechanical properties of Maraging steels as a result of hydrogen absorption. In this work, the implemented test is the Slow Strain Rate Testing (SSRT). In this standard method, the metal sample

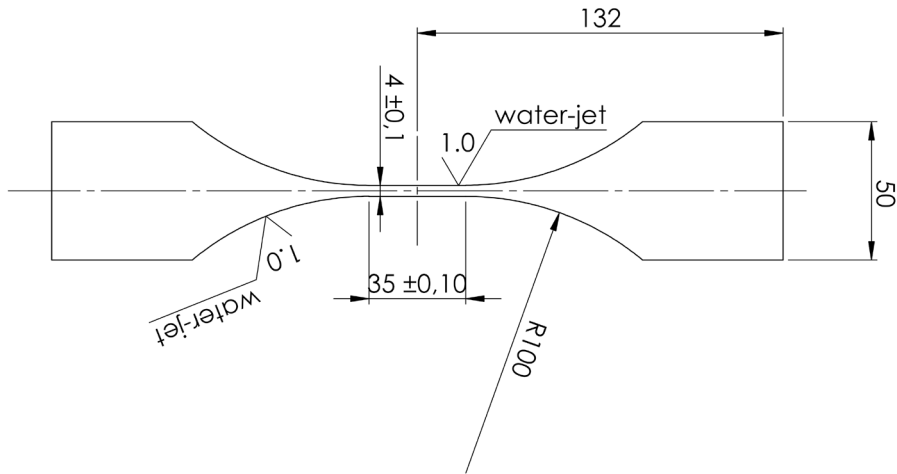


Fig. 2. Schematic design of the Maraging samples for mechanical tests.

is subjected to deformation at a constant and low speed, with values between 10^{-7} and 10^{-4} s^{-1} . The local strain rate should be low enough to prevent certain corrosion or diffusion processes to occur [ASTM (2013)].

Samples from the groups 2-4 were mechanically tested for a better understanding of the hydrogen content effect on the deterioration of mechanical properties. Samples were prepared with the schematic design shown in Fig. 2, in conformity with the ASTM E8/E8M-16a, standard [ASTM (2016)] used for traction test sample preparation.

Standard characterization of tensile properties of the samples was performed using MTS hydraulic testing machine (MTS Systems Corporation, Eden Prairie, MN USA) equipped with 100 kN load cell and MTS 634.31 F25 axial extensometer (base length 10 mm). The data acquisition system was RT3 (Trio Sistemi e Misure S.r.l., Dalmine (BG), Italy).

2.4. Surface analysis

Metallographic examination was carried out on material samples surfaces (normal to the rolling direction). Surfaces were grinded using SiC papers up to 800 grit and then mirror polished. The observation was performed using a standard optical microscope (LEICA DMI 3000 M, Leica Microsystems, Wetzlar (Germany)).

The fracture surface of the charged samples was observed using a Scanning Electron Microscope to have an indication of the hydrogen penetration profile and brittle area.

The surface condition of the blades was inspected using SEM/EDS (Energy Dispersive Spectroscopy) technique (JEOL JSM 5600LV). Fractographic investigations have been performed on the cross-section of the fractured blade using OM–Leica DM300 to define the crack pattern. Furthermore, the fracture surfaces both of the failed blades and of the fractured mechanical specimens were characterized using the same technique.

3. Results

3.1. Hydrogen charging and content measurements

The charging conditions are summarized in the first column of table 3; in the same table, the hydrogen contents of the samples are shown.

Samples from broken blades were analyzed with the same technique, and showed hydrogen concentrations ranging from 1.2 to 5.3 ppm, depending on the sampling point.

Table 3. Charging conditions and results in terms of hydrogen content C_H and UTS (Ultimate Tensile Strength).

Sample	C_H (ppm)	UTS (MPa)
Electrolytical Nickel plating	0.10	2030
Electrolytical Nickel plating	0.20	1981
Electroless Nickel plating	1.00	1934
Electroless Nickel plating	0.40	1994
Electroless Nickel plating	0.60	2078
Charged in NaOH 0.1N+10mg/l As_2O_3 at 1 mA/cm ²	3.00	1141
Charged in 3% NaCl+0.3% NH_4SCN at 0.2mA/cm ²	4.70	965
Charged in 0.1N NaOH at 1mA/cm ²	3.40	1302
Charged in 0.1N NaOH at 0.1mA/cm ²	2.10	1999
Charged in 0.1N NaOH at 0.5mA/cm ²	2.70	1678

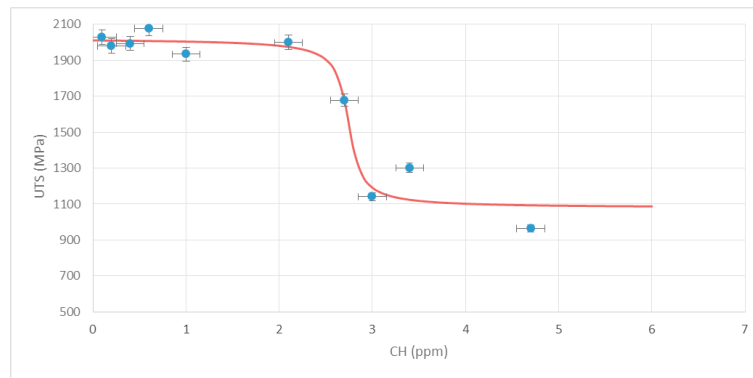


Fig. 3. UTS vs. hydrogen concentration of tested samples. The best-fit curve of the empirical model is superimposed on experimental data.

3.2. Mechanical properties

Mechanical tests samples were electrochemically hydrogen charged as described before, and the hydrogen susceptibility was assessed by performing Slow Strain Rate Testing (SSRT) according to the ASTM G-129 Standard practice. Tests were carried out in air at room temperature, with a strain rate of $4 \times 10^{-5} \text{ s}^{-1}$. Results are shown in the third column of table 3, and a wide range of Ultimate Tensile Strength (UTS) values is evident, depending on hydrogen concentration of the samples.

3.3. Data fitting

In Fig. 3 the experimental data reported in Table 3 are shown. The curve superimposed on the data represents the best fit of the UTS of all samples as a function of hydrogen concentration C_H . The best fit curve was obtained using the following 4-parameters empirical relationship:

$$UTS = a - b \cdot \arctan\left(\frac{C_H - c}{d}\right) \quad (1)$$

where the estimated values of the parameters are: $a = 1550$, $b = 301$, $c = 2.74$ and $d = 0.101$.

3.4. Fractographic analysis of samples

In the figures 4 and 5, two examples highlighting the aspects of the fracture surfaces as a function of the hydrogen content are shown.

Fractographic observations revealed, as expected, a major increment in the brittle inter-granular fracture aspect of samples when the hydrogen content increases. This is also in accordance with the experimentally detected deterioration of the mechanical properties. The crack initiation started always in the specimen external part, in correspondence

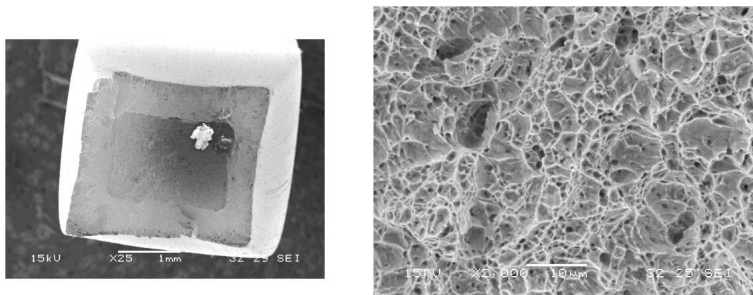


Fig. 4. SEM observation of fracture in a sample with low hydrogen content, 2.10 ppm. A ductile fracture is evident, with its characteristic dimples.

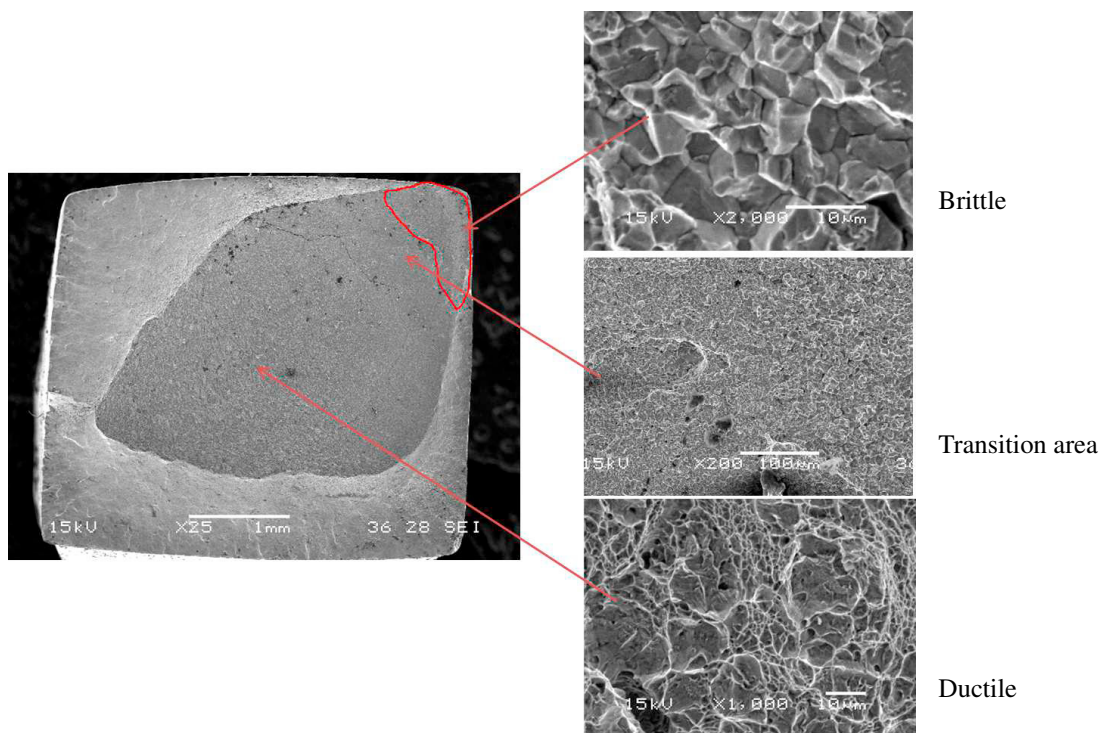


Fig. 5. SEM observation of fracture in a sample with high hydrogen content, 4.70 ppm. An inter-granular area of brittle fracture and secondary cracks are observed.

with the higher hydrogen concentration. The rest of the fracture surface remains ductile. This is a typical fracture mechanism of hydrogen embrittlement in UHSS.

3.5. Surface analysis and fractography of failed blades

All the surfaces of the nickel-plated failed blades were inspected under Scanning Electron Microscope (SEM). They showed plating discontinuities and scratches.

EDS semi-quantitative analysis on a large area of each blade shows the presence of Al, P and a high percentage of Ni (higher than its normal content in Maraging Marval 18 steel, i.e. 18%). This confirms that the Nickel plating process has been carried out for the failed blades. As an example, we consider again blade 182. Local EDS analysis on surface as received after Ni plating does not reveal high concentration of Al while EDS analysis on scratches revealed high Al concentration. Other investigated blades showed the same trend.

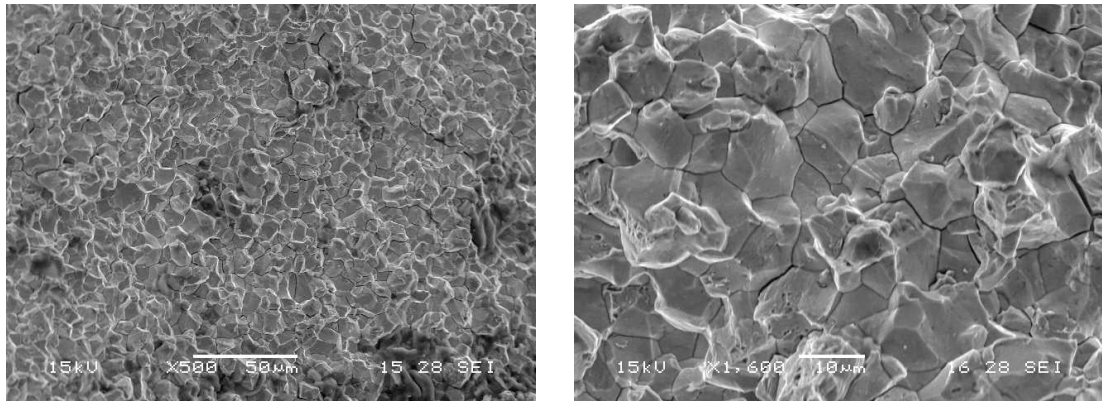


Fig. 6. Fracture surface of Blade 182.

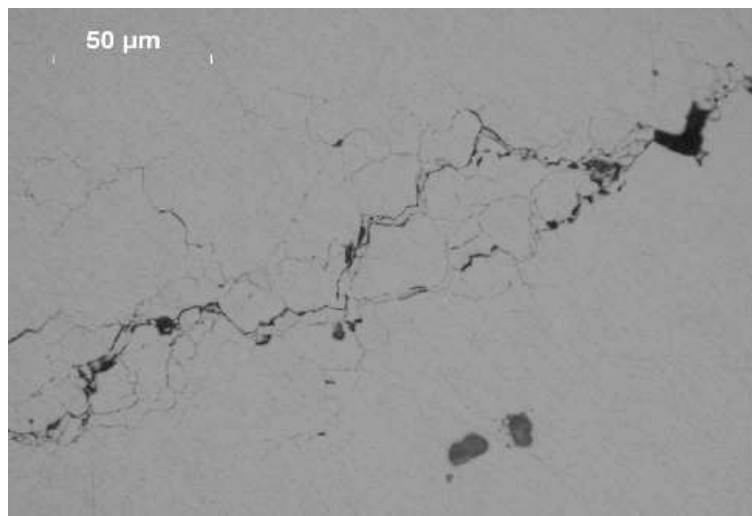


Fig. 7. Micrograph shows the crack profile normal to the failure section (with optical microscope).

Fracture surface of the failed blade was examined under SEM to determine the fracture characteristics and type. Typical inter-granular brittle fracture has been observed in all specimens along the whole specimen thickness as seen in Fig. 6. Generally, this fracture type is associated to hydrogen embrittlement phenomena. Secondary cracks were also clearly visible.

In order to study the crack profile and its propagation, the sample cross section of the same blade was prepared with ordinary metallographic procedure. By using a metallographic microscope it was examined and Fig. 7 shows a clear inter-granular crack propagation profile with characteristic secondary cracks normal to the fracture surface.

4. Conclusions and future developments

From this study one can conclude that the blades' failure is probably due to the hydrogen embrittlement mechanism. Surface analysis of failed blades revealed an inter-granular fracture with secondary cracks and high hydrogen content. Furthermore, mechanical testing results of hydrogen charged specimens are in agreement with this conclusion; in fact, the fracture aspect changed from ductile state without loss of mechanical properties (low hydrogen content) to inter-granular fracture with strong deterioration of mechanical properties. The critical hydrogen concentration, corresponding to the sharp fall of mechanical properties in the UTS-CH graph was found to be about 2.7 ppm. Fracture

surface analysis under SEM of tensile specimens confirms this finding. From these results, it is also possible to state that:

- The Maraging steel, being the highest grade of UHSS category, is very sensitive to hydrogen embrittlement phenomenon;
- some blades were subject to local corrosion phenomenon as a result of imperfections in Nickel plating, and to hydrogen exposure, due to uncontrolled atmosphere;
- some blades would have undergone incorrect nickel plating and de-hydrogenation treatments. In case of correct plating procedure, reproduced/simulated in this study, no hydrogen uptake and no mechanical properties deterioration happened. One cause could be attributed to the incorrect composition of Ni-plating bath;
- finally, the presence of surface imperfections containing high aluminum concentrations allows the creation of galvanic corrosion microcells with the consequent formation of H^+ ions resulting from local corrosive phenomena. These hydrogen ions could permeate the bulk material causing hydrogen embrittlement phenomena.

As a consequence of this study, various corrective actions have been undertaken in the handling of the blades, including the control of the hydrogen absorbed in surface treatments and the storage of the blades in a vacuum environment when Virgo experiment is not running. As far as the blade construction is concerned, it is necessary to strictly follow the plating and de-hydrogenation procedure, avoiding the exposure of plated blades to uncontrolled atmosphere for long periods. The blades should better be kept under vacuum or in dehumidified environment whenever is possible. Moreover, surface preparation before plating is considered one of the most critical steps to be controlled for UHSS. Sand blasting is to be avoided and replaced by mechanical grinding using abrasive pads (e.g. Scotch Brite or similar) as internationally recommended.

Further investigations on the estimation of the hydrogen concentration in the critical areas of the blades, taking into account the state of tension and its effect on the hydrogen diffusion, are in progress.

The results presented in this work are the starting point for the design of a new UHSS Maraging (UTS ranging from 2500 to 3000 MPa), obtainable by combining cold rolling and precipitation hardening to ensure low solubility characteristics and slow diffusivity of hydrogen, despite the improvement of the mechanical properties.

References

- ASTM, 2013. G129-00, Standard practice for slow strain rate testing to evaluate the susceptibility of metallic materials to environmentally assisted cracking. ASTM International, West Conshohocken, PA.
- ASTM, 2016. E8/E8M-16a, Standard test methods for tension testing of metallic materials. ASTM International, West Conshohocken, PA.
- Beccaria, M., Bernardini, M., Braccini, S., Bradascia, C., Cagnoli, G., Casciano, C., Cella, G., Cuoco, E., Dattilo, V., Carolis, G. D., Salvo, R. D., Virgilio, A. D., Feng, G., Ferrante, I., Fidecaro, F., Frascioni, F., Gaddi, A., Gammaitoni, L., Gennai, A., Giazotto, A., Holloway, L., Kovalik, J., Penna, P. L., Losurdo, G., Malik, S., Mancini, S., Marchesoni, F., Nicolas, J., Palla, F., Pan, H., Paoletti, F., Pasqualetti, A., Passuello, D., Poggiani, R., Popolizio, P., Punturo, M., Raffaelli, F., Rubino, V., Valentini, R., Vicere, A., Waharte, F., Zhang, Z., 1998. The creep problem in the VIRGO suspensions: a possible solution using Maraging steel. Nuclear Instruments and Methods in Physics Research Sect. A 404 (2), 455–469.
- Braccini, S., Casciano, C., Cordero, F., Corvace, F., Sanctis, M. D., Franco, R., Frascioni, F., Majorana, E., Paparo, G., Passaquieti, R., Rapagnani, P., Ricci, F., Righetti, D., Solina, A., Valentini, R., 2000. The maraging-steel blades of the Virgo super attenuator. Measurement Science and Technology 11 (5), 467–476.
- Gurewitz, G., Atzmon, N., Rosen, A., 1977. Creep and stress relaxation in 18% Ni (250) maraging steel. Metals Technology 4 (1), 62–65.
- Sha, W., Guo, Z., 2009. Maraging Steels: Modelling of Microstructure, Properties and Applications. Woodhead Publishing Series in Metals and Surface Engineering Series. CRC Press.